Interaction of Ferredoxin:NADP$^+$ Oxidoreductase with Phycobilisomes and Phycobilisome Substructures of the Cyanobacterium *Synechococcus* sp. Strain PCC 7002[†]

Carlos Gómez-Lojero,*[,‡] Bertha Pérez-Gómez,[‡] Gaozhong Shen,[§] Wendy M. Schluchter,[||] and Donald A. Bryant[§]

Departamento de Bioquímica, Centro de Investigación y Estudios Avanzados del IPN, Apartado Postal 14-740, 07000, México D.F., México, Department of Biochemistry and Molecular Biology, The Pennsylvania State University, University Park, Pennsylvania 16802, and Department of Biological Sciences, University of New Orleans, New Orleans, Louisiana 70148

Received April 30, 2003; Revised Manuscript Received August 1, 2003

ABSTRACT: The enzyme ferredoxin-NADP$^+$ oxidoreductase (FNR) from *Synechococcus* sp. PCC 7002 has an extended structure comprising three domains (FNR-3D) (Schluchter, W. M., and Bryant, D. A. (1992) *Biochemistry 31*, 3092−3102). Phycobilisome (PBS) preparations from wild-type cells contained from 1.0 to 1.6 molecules of FNR-3D per PBS, with an average value of 1.3 FNR per PBS. A maximum of two FNR-3D molecules could be specifically bound to wild-type PBS via the N-terminal, CpcD-like domain of the enzyme when exogenous recombinant FNR-3D (rFNR-3D) was added. To localize the enzyme within the PBS, the interaction of PBS and their substructures with rFNR-3D was further investigated. The binding affinity of rFNR-3D for phycocyanin (PC) hexamers, which contained a 22-kDa proteolytic fragment derived from CpcG, the L_{RC}^{27} linker polypeptide, was higher than its affinity for PC hexamers containing no linker protein. PBS from a *cpcD3* mutant, which lacks the 9-kDa, PC-associated rod linker, incorporated up to six rFNR-3D molecules per PBS. PBS of a *cpcC* mutant, which has peripheral rods that contain single PC hexamers, also incorporated up to six rFNR-3D molecules per PBS. Direct competition binding experiments showed that PBS from the *cpcD3* mutant bound more enzyme than PBS from the *cpcC* mutant. These observations support the hypothesis that the enzyme binds preferentially to the distal ends of the peripheral rods of the PBS. These data also show that the relative affinity order of the PC complexes for FNR-3D is as follows: $(\alpha^{PC}\beta^{PC})_6-L_R^{33} > (\alpha^{PC}\beta^{PC})_6-L_{RC}^{27} > (\alpha^{PC}\beta^{PC})_6$. The data suggest that, during the assembly of the PBS, FNR-3D could be displaced to the periphery according to its relative binding affinity for different PC subcomplexes. Thus, FNR-3D would not interfere with the light absorption and energy transfer properties of PC in the peripheral rods of the PBS. The implications of this localization of FNR within the PBS with respect to its function in cyanobacteria are discussed.

Ferredoxin-NADP$^+$ oxidoreductase (FNR;[1] EC 1.18.1.2) transfers electrons from ferredoxin (or flavodoxin) to NADP$^+$ to generate NADPH (*1*). In eukaryotes, the nuclear-encoded, chloroplast-targeted enzyme is processed to a mature length of ∼314 amino acids; its three-dimensional structure has been determined, and it contains two domains: an FAD-binding domain and an NADP$^+$-binding domain (*2*−*4*). In the cyanobacterium *Synechococcus* sp. PCC 7002, FNR was shown to possess a third N-terminal domain that localized the enzyme to the phycobilisomes (PBS) (*5*), and subsequent studies similarly showed the actual mass of FNR in diverse cyanobacteria to be 45−50 kDa (*5*−*9*). With the exception of *Gloeobacter violaceous* PCC 7421, the predicted sequences of all cyanobacterial *petH* genes, encoding FNR,

[†] This study was supported by Grant GM31625 from The National Institutes of Health (D.A.B.) and CONACYT-Mexico (ref. no. 981072) and Fulbright (grant no. 23653) U.S.A. (C.G.L.).

* To whom correspondence should be addressed. Telephone: (5255) 5747-7082. Fax: (5255) 5747-7083. E-mail: cgomez@enigma.red.cinvestav.mx.

[‡] Centro de Investigación y Estudios Avanzados del IPN.

[§] The Pennsylvania State University.

[||] University of New Orleans.

[1] Abbreviations: APC, allophycocyanin; *apcAB*, gene encoding the α and *β* subunits of allophycocyanin; *apcC*, gene encoding the 8-kDa core linker polypeptide; a.u., absorbance units; *cpcBA*, genes encoding the α and *β* subunits of phycocyanin; *cpcC*, gene encoding the 33-kDa rod linker polypeptide; *cpcD*, gene encoding the 9-kDa rod linker polypeptide; *cpcG*, gene encoding the 27-kDa rod-core linker polypeptide; DCPIP, dichlorophenol-indophenol; DMF, dimethyl-formamide; EDTA, ethylenediamine tetraacetic acid; FNR, ferredoxin-NADP$^+$ oxidoreductase; FNR-2D, FNR containing only the two catalytic domains; FNR-3D, FNR containing three domains (the CpcD-like domain and two catalytic domains); LB, Luria−Bertani medium; L_C^8, core linker polypeptide of 8 kDa; L_{CM}^{99}, ApcE, the 99-kDa core membrane linker phycobiliprotein; L_R^9, the 9-kDa, phycocyanin-associated rod linker polypeptide; L_R^{33}, CpcC, the 33-kDa rod linker polypeptide; L_{RC}^{27}, CpcG, the 27-kDa rod core linker polypeptide; L_{RC}^{22}, a 22-kDa proteolytic fragment derived from CpcG; IPTG, isopropyl-*O*-D-thio-galactopyranoside; PAGE, polyacrylamide gel electrophoresis; PBP(s), phycobiliprotein(s); PBS, phycobilisome(s); PC, phycocyanin; *petH*, gene encoding FNR-3D; PMSF, phenyl-methylsulfonyl fluoride; rFNR-2D, recombinant FNR of two domains; rFNR-3D, recombinant FNR of three domains; SDS, sodium dodecyl sulfate; WCE(s), whole-cell extract(s).

10.1021/bi0346998 CCC: $25.00 © 2003 American Chemical Society
Published on Web 10/30/2003

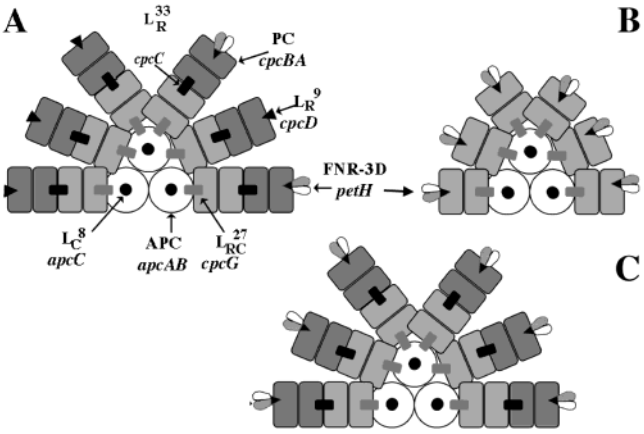

FIGURE 1: Schematic models of phycobilisomes. (A) Hemidiscoidal PBS with tricylindrical APC core of *Synechococcus* sp. PCC 7002. Genes encoding various components of these PBS are indicated with their translation products. (B) Schematic model for PBS isolated from the *cpcC* mutant strain after exposure to saturating amounts of rFNR-3D. (C) Schematic model for PBS isolated from the *cpcD3* mutant strain after exposure with saturating amounts of rFNR-3D.

have lengths of 386-440 amino acids, and these sequences correspond to a protein containing three domains (here denoted FNR-3D; refs *5*, *6*, and *10*−*13*).

The N-terminal extension, which comprises the third domain of FNR-3D of *Synechococcus* sp. PCC 7002, is 78% similar to CpcD, the 9-kDa phycocyanin (PC)-associated, rod-capping, linker polypeptide, L_R^9, of PBS (ref *5* and see Figure 1A). Thus, it was proposed that the enzyme is bound to the core-distal ends of the peripheral rods of PBS (*5*). However, the N-terminal extension of FNR-3D is also similar to other PBS-associated linker proteins. For example, the N-terminal domain of *Synechocystis* sp. PCC 6803 FNR is 69% similar to the C-terminal domain of CpcC, the PC-associated rod linker polypeptide L_R^{33}, and 65% similar to ApcC, the allophycocyanin (APC)-associated, core linker polypeptide L_C^8 (*14*). In *Synechocystis* sp. PCC 6803, evidence has been presented purporting to show that FNR-3D is bound to the core-proximal PC hexamer of the peripheral, PC-containing rods of the PBS (*14*). The linker polypeptides of PBS are believed to be located mainly in the central cavity of the toroid-shaped phycobiliproteins; this localization is supported by the X-ray structure of APC with the L_C^8 linker (*15*). It is possible that linker polypeptides somehow interact to form a scaffold-like structure within the PBS (*16*). Whether or not this is the case, it is possible to distinguish various PC subassemblies specifically by their state of aggregation and by their attached linker polypeptides (*17*−*19*). All of these observations prompted this study of the interactions of FNR-3D with various PBS substructures to establish absolutely the localization of FNR-3D within the PBS.

Synechococcus sp. PCC 7002 is an ideal organism for a detailed study of the interaction of FNR-3D with PBS substructures. Its PBS are composed of only 12 structural polypeptides (see model in Figure 1A), and only single genes encode each polypeptide (*17*). The DNA sequences of the genes encoding all of the subunits are known, and all of the structural genes except that for the essential enzyme FNR have been inactivated to produce null mutants (*17*−*20*). For example, the *cpcC* mutant produces PBS whose peripheral rods contain a single PC hexamer (Figure 1B), and the *cpcD3* mutant produces PBS whose peripheral rods are variable in length and are not terminated by CpcD (Figure 1C). It is also possible to purify large amounts of *Synechococcus* sp. PCC 7002 FNR-3D by overproducing the protein in *Escherichia coli* (*8*).

Even though the principal function of FNR is to catalyze the terminal step of the electron transport chain in organisms performing oxygenic photosynthesis (*1*), other functions for FNR have been proposed. It has been suggested that FNR participates in cyanobacterial respiration (*21*), specifically as an NADPH dehydrogenase (*22*), and in cyclic electron transport. The role of FNR-3D in cyclic electron transport has been suggested by two observations. First, the reduction of $P700^+$ is not observed when the third domain of FNR is deleted in *Synechocystis* sp. PCC 6803. Second, *Synechocystis* sp. PCC 6803 is unable to adapt to high-salt stress, a condition that creates a high demand for ATP, when its FNR lacks the N-terminal domain (*23*). Recently, a role as a ferredoxin-plastoquinone reductase has been proposed for the FNR-cytochrome b_6f complex in cyclic electron transport in chloroplasts (*24*). To fulfill all of these functions, it is important that FNR be localized in close proximity to the membrane components that participate in cyclic electron transport and respiration. Characterization of the structural relationships among PBS components, thylakoid membrane components, and FNR-3D could provide information on the role(s) of FNR-3D in cyclic electron transport.

In this paper, we show that the N-terminal domain of FNR-3D is essential for the binding of the enzyme to PBS. Under saturating enzyme conditions, a wild-type PBS binds approximately two molecules of FNR. Using wild-type PBS, PBS isolated from mutants of *Synechococcus* sp. PCC 7002 (see models in Figure 1), and PC-containing subcomplexes, the affinity of the FNR-3D for the various PC complexes has the following order: $(\alpha^{PC}\beta^{PC})_6-L_R^{33} > (\alpha^{PC}\beta^{PC})_6-L_{RC}^{27} > (\alpha^{PC}\beta^{PC})_6$. This hierarchy of affinities supports the original hypothesis that FNR is localized at the distal ends of the peripheral rods of PBS (*5*) and suggests that FNR-3D is displaced to the ends of the rods during assembly.

EXPERIMENTAL PROCEDURES

Growth Conditions for Cyanobacterial Cultures. Synechococcus sp. PCC 7002 was grown photoautotrophically in medium A^+ (*25*) under continuous illumination from cool-white fluorescent lamps at an intensity of ~250 μE m^{-2} s^{-1}. Cell suspensions were bubbled with 2−5% (v/v) CO_2 in air. Cells were grown in 25-mL and 1.8-L liquid cultures at 38 °C or at room temperature (~22 °C), respectively. The same growth medium with the addition of 100 μg of kanamycin mL^{-1} was used for mutant strains. Mid- to late-exponential phase cells were used for all experiments.

Preparation of Whole-Cell Extracts and Isolation of PBS by Sucrose Density Gradient Centrifugation. *Synechococcus* sp. PCC 7002 cells were harvested by centrifugation, washed, and resuspended in 0.65 M Na^+/K^+-phosphate buffer, pH 8.0, containing 1 mM NaN_3, 20 μg of PMSF mL^{-1}, and 10 mM Na-EDTA. Whole-cell extracts (WCEs) were produced by disrupting cells by four successive passes through a French pressure cell operated at 18 000 psi. Triton X-100 was added to the WCE to a concentration of 1.2% (v/v).

The solution was gently stirred for 30 min at room temperature and then centrifuged for 30 min at 23 500*g*. All sucrose gradients were prepared in 0.75 M Na^+/K^+-phosphate buffer, pH 8.0, containing 10 mM EDTA, 1 mM NaN_3, and 20 μg of PMSF mL^{-1}. All samples were added in 0.65 M Na^+/K^+-phosphate buffer pH 8.0 in the presence of the same inhibitors as above. Sucrose gradients were prepared as previously described (*26*). The ultracentrifugation was carried out for 12 h at 20 °C at 65 000*g* in a Beckman Ti 60 rotor. The fractions containing PBSs were collected from the step gradients and assayed for sucrose concentration with an Abbé refractometer. Fractions were also analyzed for absorbance at 630 and 650 nm, for diaphorase activity, and by SDS−PAGE.

Insertional Inactivation of the cpcC Gene in Synechococcus sp. PCC 7002. For the construction of a *cpcC* mutant, a derivative of pAQPR2 was used in which the *cpcC* gene was insertionally inactivated. Plasmid pAQPR2 harbors a 3.0-kb *Hind*III fragment encoding *cpcBAC* from *Synechococcus* sp. PCC 7002 inserted into vector pBR325; the insert is oriented oppositely from the insert in pAQPR1 described previously (*19*). The insert encodes the *cpcB* and *cpcA* genes, encodes the β and α subunits of the phycocyanin, respectively, as well as the *cpcC* gene, which encodes the 33-kDa rod-linker polypeptide (L_R^{33}) (*19*). The *cpcC* gene was inactivated by inserting a 1.32-kb *Sal*I fragment, derived from plasmid pRL161 and encoding the *aphII* gene of Tn*5*, which confers resistance to the antibiotic kanamycin, into a unique *Xho*I site within the *cpcC* coding region (*19*). This construct was used to transform *Synechococcus* sp. PCC 7002 cells. The transformants were screened on A^+ plates supplemented with kanamycin. Full segregation of the *cpcC* gene interruption was verified by PCR analysis (data not shown).

Expression and Purification of the rFNR-3D. For overexpression of the *petH* gene encoding the rFNR-3D protein, the *Synechococcus* sp. PCC 7002 *petH* gene was cloned into the expression vector pET3a (Novagen, Madison, WI), resulting in the pET3a*::petH*1.6A expression plasmid. Cells of *E. coli* strain BL21 (DE3) (*5*) harboring pET3a*::petH*1.6A were grown in LB medium with addition of 50 nM riboflavin and 100 μg mL^{-1} ampicillin. Induction of FNR-3D protein expression was achieved by addition of 0.5 mM IPTG. Cells containing the overproduced FNR protein were harvested and resuspended in 0.1 M Tris-HCl pH 8.0, 10 mM EDTA, and 0.1 M NaCl. Cells were broken by ultrasonic disruption or by two passages through the French press at 18 000 psi. Unbroken cells, debris, and membranes were removed by low-speed centrifugation at 6400*g* at 4 °C. The supernatant was slowly adjusted to 60% of saturation with solid $(NH_4)_2SO_4$ and stirred for 30 min. The rFNR-3D was pelleted by centrifugation at 23 500*g* for 20 min. To obtain rFNR-2D, the supernatant from the 60% $(NH_4)_2SO_4$ fractionation was adjusted to 90% of saturation with solid NH_4SO_4 and incubated and centrifuged as stated previously. Each pellet was suspended in 50 mM Tris-HCl pH 8.0, 10 mM EDTA, and 0.1 M NaCl and dialyzed against the same buffer. The dialyzed sample was loaded onto a Cibacron blue column (25 × 1.5 cm) and washed with loading buffer. The rFNR-3D was eluted with a linear NaCl gradient (0.1−1 M; 400 mL) prepared with 50 mM Tris-HCl buffer pH 8.0 supplemented with 10 mM EDTA, 1 mM NaN_3, and 20 μg of PMSF mL^{-1}. The FNR concentration in each 5.0-mL column fraction was determined by using the ϵ_{458} of 9.5 mM^{-1} cm^{-1} (*27*). The enzyme had an apparent molecular mass of 45 kDa and was judged to be >95% pure by SDS−PAGE. FNR-2D was purified by a similar procedure.

Isolation of Phycocyanin from Phycobilisomes. The isolation of PC complexes from PBS of *Synechococcus* sp. PCC 7002 was performed as described (*28*). The first fraction eluted was PC, and the second fraction contained the PC-22-kDa linker complex, with the characteristic absorption spectrum of complex PC-L_{RC}^{27} (*28*).

Absorption Spectra. Absorption spectra were recorded with a DW2 Aminco spectrophotometer or with a Beckman model DU 650 spectrophotometer. The molar extinction coefficient at 630 nm used for the PBS from the wild type and *cpcD3* mutant strains was 3.3×10^7 M^{-1} cm^{-1}, calculated using extinction coefficients at 630 nm of PC and APC and the PBS model for *Synechococcus* sp. PCC 7002 (*17*). The ϵ_{630} for PC ($\alpha\beta$) protomers was 395 mM^{-1} cm^{-1} and was 134 mM^{-1} cm^{-1} for APC ($\alpha\beta$) protomers (*26*). The PBS model used has 36 APC ($\alpha\beta$) protomers (i.e., a tricylindrical core) and two PC $(\alpha\beta)_6$ hexamers in each of six peripheral rods, for a total of 72 ($\alpha\beta$) protomers of PC (ref *17*, see also Figure 1A,C). For PBS from the wild type and the *cpcD3* mutant, an ϵ_{650} of 1.98×10^7 M^{-1} cm^{-1} was calculated by multiplying the ϵ_{630} by 0.57, which is the ratio of absorption at 650 and 630 nm obtained from their absorption spectra. Using a model of 36 APC ($\alpha\beta$) protomers and 36 PC ($\alpha\beta$) protomers (ref *19* and also see Figure 1B), the extinction coefficients calculated for PBS of the *cpcC* mutant were 1.9×10^7 M^{-1} cm^{-1} at 630 nm and 1.68×10^7 M^{-1} cm^{-1} at 650 nm. The latter value was calculated from the spectroscopic ratio 650/630 nm = 0.88 determined from the absorption spectrum. To calculate the concentration of PBS in mixtures from the *cpcC* and *cpcD3* mutant strains, simultaneous equations were solved using the absorbance values at 630 and 650 nm together with the extinction coefficients for each as described previously. Finally, the extinction coefficient used for PC $(\alpha\beta)_6$ hexamers at 630 nm was 1.5×10^6 M^{-1} cm^{-1}, and that used for the hexameric PC-L_{RC}^{22} complex was 1.8×10^6 M^{-1} cm^{-1} at 638 nm (*28*).

Activity Measurements of FNR. FNR diaphorase activity was measured as the reduction of DCPIP by NADPH and was followed at 600 nm using a 0.5 cm path-length cell containing 50 mM Tris-HCl pH 8.0, 100 μM DCPIP, and 100 μM NADPH against a reference cell containing the same buffer with 50 μM DCPIP (*29*). The turnover number of the diaphorase activity for rFNR-3D, which was used to calculate the FNR concentration of the gradient fractions, was determined by calculating the difference between the total activity of the centrifuge tube, in which rFNR-3D was added, minus the total basal activity of the tube, divided by the nmoles of enzyme added. A turnover number was determined for each experiment.

SDS−PAGE Analyses. SDS−PAGE analyses were performed on 14% (w/v) polyacrylamide slab gels (*30*). The proteins were stained with Coomassie blue R-250. Densitometric scans were performed with a Pharmacia LKB UltroScan XL and analyzed with the Program GSXL version 2.1. The relative molar amounts of protein per band were obtained as described (*31*). The scaling factors used were 9.7 for L_{CM}; 4.5 for FNR-3D; 3.3 for L_R^{33}; 2.7 for L_{RC}^{27}; 1.8 for all PBPs; and 0.9 for L_R^9 and L_C^8. All stoichiometries

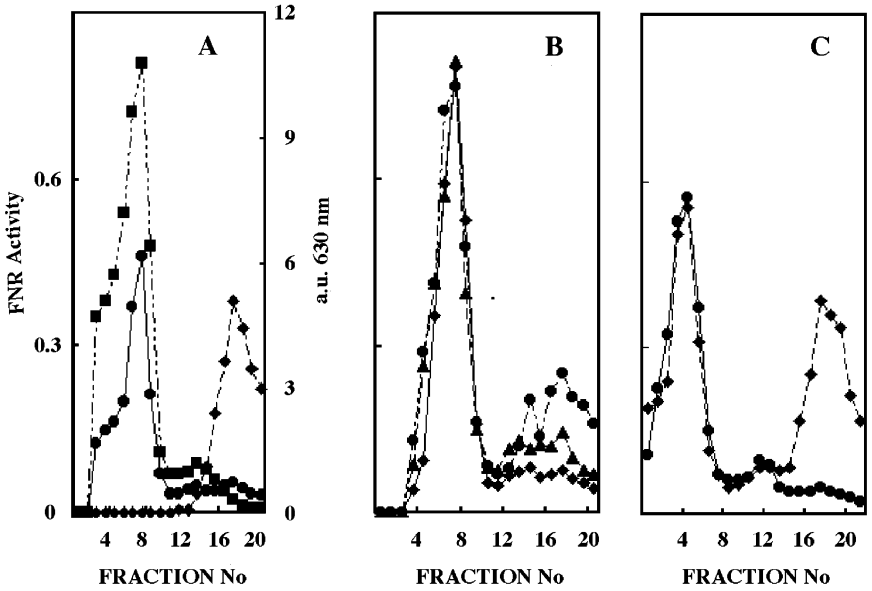

FIGURE 2: Sucrose density gradient analysis of phycobilisomes from wild-type *Synechococcus* sp. PCC 7002. FNR activity is expressed as μmol of DCPIP min^{-1} mL^{-1}. Panel A shows the patterns of fractions obtained from two different sucrose gradients. One gradient was loaded with WCE from *Synechococcus* sp. PCC 7002 wild-type cells after solubilization with Triton X-100. The FNR activity (●) and the absorbance at 630 nm (■) of each fraction are indicated. The second gradient was loaded with only 2.1 nmol of purified rFNR-3D (♦ FNR activity). Panel B shows the FNR activity (expressed as μmol of DCPIP min^{-1} mL^{-1}) present in fractions collected from three different sucrose gradients. Increasing amounts of rFNR-3D (1.05 (■), 2.1 (▲), and 3.15 (●) nmol) were added to three equivalent aliquots of a Triton X-100-solubilized WCE from the wild-type strain of *Synechococcus* sp. PCC 7002 prior to loading on the gradients. Panel C shows the FNR activity in fractions collected from gradients containing WCE from the wild-type strain of *Synechococcus* sp. PCC 7002 solubilized by Triton X-100 (●) alone or after incubation with rFNR-2D (3 μmol of DCPIP min^{-1} mL^{-1}, or ~1 nmol of rFNR-2D) (◆). The scale for FNR activity for panels B and C is the same as that in panel A.

were calculated relative to six molecules of the 27-kDa L_{RC}^{27} linker polypeptide (*17)*; the L_{RC}^{27} linkers connect the six peripheral rods of the PBS to the core.

Determination of the Stoichiometries of FNR in Wild-Type PBS. Six centrifuge tubes were prepared with identical sucrose gradients. The blue, PBS-containing supernatant (25 mL; 9.3 a.u. at 630 nm) in 0.65 M Na^+/K^+-phosphate buffer, pH 8.0, containing 1 mM NaN_3, 20 μg of PMSF mL^{-1}, and 10 mM Na-EDTA obtained after low-speed centrifugation of a wild-type WCE was split into five equal aliquots of 5 mL. No additions were made to two aliquots that served as controls of the basal diaphorase activity in the gradient (Figure 2A). rFNR-3D was added (1.05, 2.1, and 3.15 nmol, respectively) to the three remaining aliquots. A sixth sucrose gradient was used to determine the sedimentation behavior of 2.1 nmol of rFNR-3D alone. After centrifugation, 21 fractions of 1.2 mL were collected from bottom to top from each centrifuge bottle using a peristaltic pump and tubing fitted with a capillary tip. The turnover number of the diaphorase activity for the rFNR-3D, which was used to calculate the FNR concentration for this experiment, was obtained as described earlier.

RESULTS

FNR-3D is Associated With the PBS. Figure 2A shows the combined sedimentation profiles of a sucrose gradient, which had been loaded with the blue-colored, PBS-containing supernatant from the detergent solubilized WCE of *Synechococcus* sp. PCC 7002, and a gradient that had been loaded with the purified rFNR-3D from *Synechococcus* sp. PCC 7002. The diaphorase activity profile for the WCE alone (Figure 2A, circles) shows three obvious peaks corresponding to fractions 8, 14, and 18. The most rapidly sedimenting fraction contained the PBS and 78% of the FNR activity. The middle peak contained a mixture of comigrating phycobiliproteins with apparent masses of ~250 kDa, and the most slowly sedimenting peak (fraction 18) contained uncomplexed FNR since this fraction corresponds to the peak position of purified rFNR-3D (Figure 2A, diamonds). To determine if the two more slowly sedimenting fractions of enzyme activity were artifacts of the purification procedure, or if these fractions truly were present in fresh WCEs, identical sucrose gradients were analyzed to compare the sedimentation profile of FNR activity for crude PBS and previously purified PBS. Both of these samples showed the same three peaks of FNR activity obtained previously (data not shown). These sedimentation profiles indicated that some continuing dissociation of the PBS occurred during the second centrifugation. It was subsequently found that, by reducing the number of passages of cells through the French press, cell breakage and the yield of soluble proteins was diminished. However, ammonium sulfate fractions of such WCEs indicated that only ~3% of the total diaphorase activity was found in the 40% saturated ammonium-sulfate supernatant, whereas the majority (97%) of the activity was found associated with the pellet fraction containing PBS (data not shown). Thus, this shortened procedure led to a much greater retention of FNR on the PBS. On the basis of these observations, we conclude that 97% or more of the FNR activity is associated with PBS in wild-type *Synechococcus* sp. PCC 7002 cells under standard growth conditions.

Experiments to determine the interaction between the PBS and the different concentrations of rFNR-3D were performed to establish the saturability and stoichiometry of the binding of exogenously added rFNR-3D to PBS. The experiments in Figure 2B show that rFNR-3D binds to the PBS and that

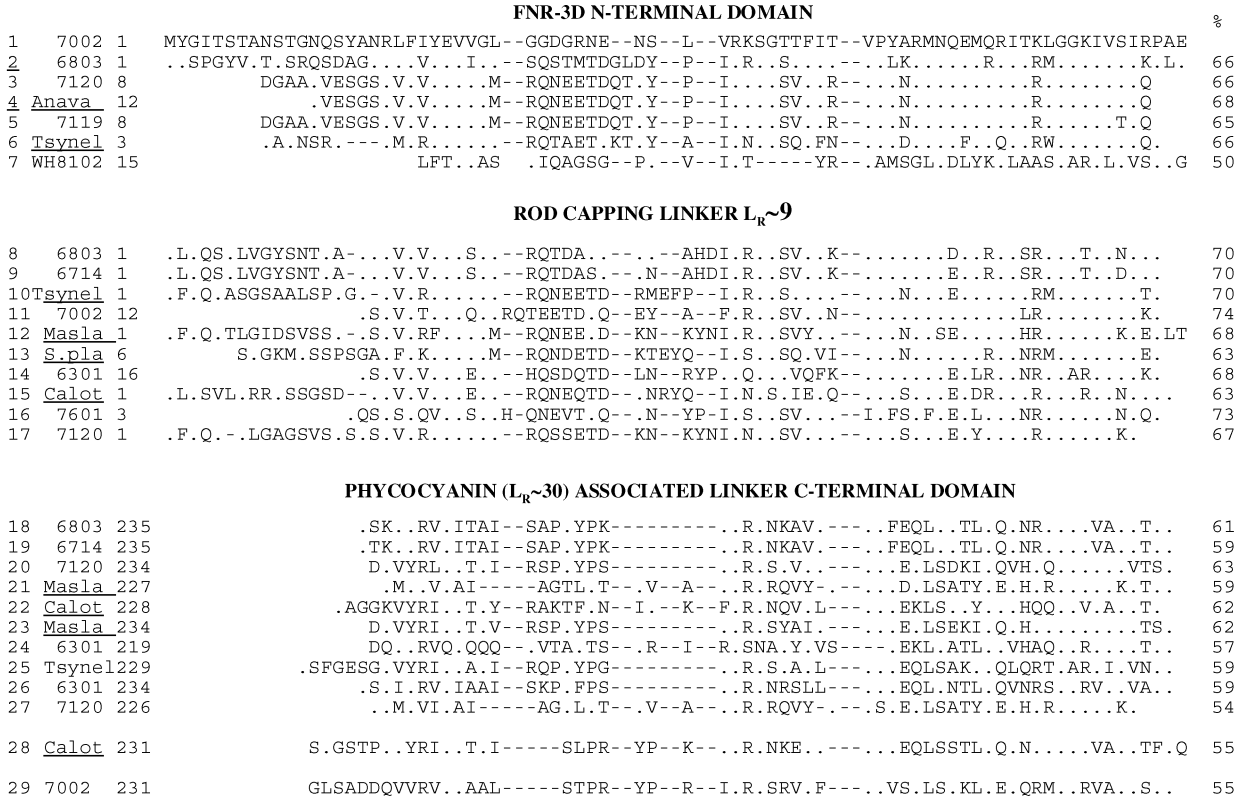

FIGURE 3: Amino acid sequence comparison of the N-terminal domain of FNR-3D with cyanobacterial linker proteins. Dots indicate identical amino acid, dashes indicate insertions/deletions introduced to maximize the sequence similarity, and the percent similarity is shown at the right. The FNR N-terminal domain sequences shown are derived from the following organisms: [1] *Synechococcus* sp. PCC 7002 (*5*); [2] *Synechocystis* sp. PCC 6803 (*10*); [3] *Nostoc* sp. PCC 7120 (*13*); [4] *Anabaena variabilis* (GI: 2498066); [5] *Anabaena* sp. PCC 7119 (*12*); [6] *Thermosynechococcus elongatus* (*11*); and [7] *Synechococcus* sp. WH 8102 (GI: 23133339). The amino acid sequences of peripheral rod-capping linker polypeptides (CpcD) are derived from the following organisms: [8] *Synechocystis* sp. PCC 6803, $L_R^{8.9}$ (*10*); [9] *Synechocystis* sp. PCC 6714 (GI: 18147769); [10] *Thermosynechococcus elongatus*, L_R^9 (GI: 1709964); [11] *Synechococcus* sp. PCC 7002, L_R^9 (*19*); [12] *Mastigocladus laminosus*, $L_R^{8.9}$ (*32*); [13] *Spirulina platensis* (GI: 5726480); [14] *Synechococcus* sp. PCC 6301, L_R^9 (*33*); [15] *Calothrix* sp. $L_R^{9.7}$ (*34*); [16] *Calothrix* sp. PCC 7601, $L_R^{8.1}$ (*35*); and [17] *Nostoc* sp. PCC 7120, $L_R^{8.9}$ (*13*). Amino acid sequences of the C-terminal domain of PC-associated linkers (CpcC) were derived from the following organisms: [18] *Synechocystis* sp. PCC 6803, $L_R^{32.1}$ (*10*); [19] *Synechocystis* sp. PCC 6714 (GI: 18147768); [20] *Nostoc* sp. PCC 7120 (*13*); [21] *Mastigocladus laminosus*, $L_R^{34.5}$ (*32*); [22] *Calothrix* sp., $L_R^{32.1}$ (*36*); [23] *Mastigocladus laminosus*, $L_R^{32.1}$ (*32*); [24] *Synechococcus* sp. PCC 6301, L_R^{30} (*33*); [25] *Thermosynechococcus elongatus*, L_R^{32} (GI: 1709956); [26] *Synechococcus* sp. PCC 6301, L_R^{33} (*33*); [27] *Nostoc* sp. PCC 7120, $L_R^{34.5}$ (*13*); [28] *Calothrix* sp., L_R^{39} (*34*); and [29] *Synechococcus* sp. PCC 7002 (*19*).

it is possible to saturate the FNR binding sites on PBS with rFNR-3D. The amount of enzyme bound to PBS increased significantly after reconstitution with the rFNR-3D, even after the addition of only 1.05 nmol of rFNR-3D. The level of FNR bound remained almost constant when PBS were mixed with 2.10 and 3.15 nmol of rFNR-3D. The excess enzyme was recovered in the upper part of the gradients. These results show that there are a limited number of sites for FNR-3D in PBS. The calculated stoichiometry of FNR per PBS was ~2 in these experiments. This result agrees with previous estimates for both *Synechococcus* sp. PCC 7002 (*5*) and *Synechocystis* sp. PCC 6803 (*14*). The initial FNR level in the wild-type PBS varied from 1.0 to 1.6 per PBS with an average of 1.3 molecules of FNR per PBS.

PBS were also incubated with a recombinant, two-domain enzyme (FNR-2D) that lacks the N-terminal, CpcD-like domain to show that the binding assay was specific for FNR-3D. This form of FNR is spontaneously produced by proteolysis in *E. coli*. Figure 2C compares the sedimentation profiles of wild-type PBS and the same PBS after incubation with FNR-2D. The faster sedimenting fractions also contained the diaphorase activity associated with the PBS, but no increase in the amount of FNR activity associated with the PBS was observed after incubation with FNR-2D. Likewise, the intermediate fraction, which contains the activity associated with dissociated PC complexes, did not show an increase in diaphorase activity after incubation with FNR-2D. Only the most slowly sedimenting zone, containing uncomplexed, FNR-2D, showed an increase in diaphorase activity. The data in Figure 2B,C show that the binding of FNR-3D to PBS can be saturated and that PBS do not bind FNR-2D lacking the CpcD-like domain, strongly supporting the hypothesis that the N-terminal, CpcD-like domain with similarity to L_R^9 is responsible for the binding of FNR-3D to PBS.

The N-terminal domain of FNR-3D of *Synechococcus* sp. PCC 7002 has sequence similarity with the linker polypeptides of PBS from numerous cyanobacteria. As shown in Figure 3, the amino acid sequence of this domain consists of 75 amino acids with very high sequence similarity to the peripheral rod-capping linkers associated with PC (L_R^9, 69%). A region of approximately 60 amino acids also has high sequence similarity to the C-terminal region of 30-kDa, PC-associated rod linkers (L_R ~30, 59%). A region of ap-

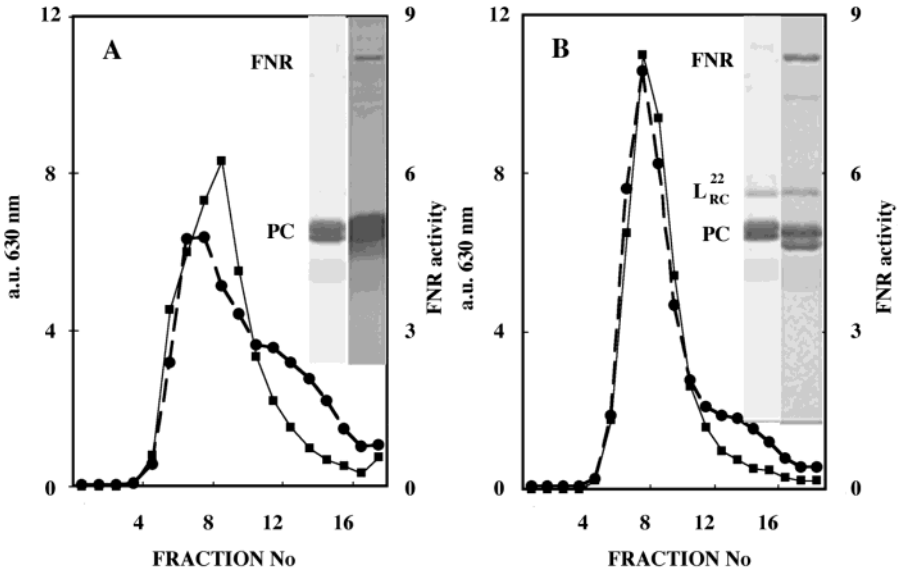

FIGURE 4: Sucrose density gradient analysis of PC hexamers and PC-L_{RC}^{22} complexes after incubation with rFNR-3D. Panel A shows the properties of fractions collected from a sucrose gradient loaded with PC $(\alpha\beta)_6$ hexamers after mixing with 18.4 nmol of rFNR-3D. Panel B shows the profile from a sucrose gradient loaded with the PC-$(\alpha^{PC}\beta^{PC})_6-(L_{RC}^{22})_1$ complex after mixing with 18.4 nmol of rFNR-3D. PC was monitored at 630 nm (■), and FNR activity (●) is expressed as μmol of DCPIP min^{-1} mL^{-1}. Samples (50 μg of total protein) from peak activity fractions of the experiments shown in Figure 3A,B were separated by SDS−PAGE. Insets: electrophoretograms of PC and PC-L_{RC}^{22} linker complexes before (left lane) and after (right lane) incubation with rFNR-3D. The identities of the polypeptides are indicated at the left of the electrophoretograms.

proximately 35 amino acids has sequence similarity to the small, APC-associated core linkers (L_C^8, 59%). Since the CpcD proteins are typically 70−85 amino acids, the similarity spans nearly the entire sequence of this linker class. However, since rod linkers of the CpcC class are typically 273−291 amino acids long, the similarity is confined only to the C-terminus of this linker class. The similarity to the L_C^8 linker class (*apcC* gene products) only corresponds to about half of the molecule (37 out of 67 amino acids). Significantly, the region of similarity forms secondary structure elements, which are known to form direct contacts with the β subunits of the APC (*15*). On the basis of these sequence similarities, the interactions of FNR-3D with different phycobiliprotein-linker complexes, including PC L_R^{33} and PC-L_{RC}^{27}, were studied to establish which PC-containing complexes had the highest affinity for FNR-3D within the PBS.

Sucrose Gradient Centrifugation Analysis of Phycocyanin Complexes Isolated from Synechococcus sp. PCC 7002 After Incubation with rFNR-3D. Two fractions containing PC were purified from PBS isolated from wild-type *Synechococcus* sp. PCC 7002 cells. One fraction contained a 22-kDa-linker polypeptide fragment (L^{22}) bound to PC, and the other one contained only PC. The shape of the absorption spectrum of PC-L^{22} (data not shown) with a sharp peak at 638 nm demonstrates that $(\alpha^{PC}\beta^{PC})_6-(L^{22})_1$ is a complex between PC and a proteolytic fragment derived from the L_{RC}^{27} polypeptide (*28*, *37*, *38*). Figure 4A shows that two zones of diaphorase activity could be resolved on a sucrose density gradient after incubation of 19.2 nmol of rFNR-3D with 4 mL of phycocyanin (OD_{630} = 10). In this experiment, a 1.4-fold excess of PC, calculated as $(\alpha\beta)_6$ hexamers, was added over the rFNR-3D. The first zone (fractions seven to 10) of diaphorase activity (Figure 4, closed circles) matches the first half of the absorbance profile (Figure 4, closed squares) for PC, which has its maximum in fraction 10. The stoichiometry in fractions seven to 10, estimated as rFNR-3D:$(\alpha^{PC}\beta^{PC})_6$, was 0.52 ± 0.1. The second zone (fractions 13−17) of diaphorase activity corresponds to free rFNR-3D. Figure 4B shows the absorbance and diaphorase activity profiles after sucrose density gradient centrifugation of a mixture of rFNR-3D with the PC-L_{RC}^{22} complex. There is a much closer correspondence between the distribution of FNR activity (Figure 4B, closed circles) and the 630 nm absorption (Figure 4B, closed squares) when compared to the profile in Figure 4A. The distributions of both activity and absorbance are narrower and more symmetric, which suggests that only PC hexamers are present. According to the activity measured for fractions seven to 10, there is 0.62 ± 0.08 FNR-3D per $(\alpha^{PC}\beta^{PC})_6-(L_{RC}^{22})_1$ complex. To establish further the relative affinities of the two types of PC complexes for rFNR-3D, smaller amounts of enzyme (4.8 and 9.6 nmol) were incubated with the PC complexes. The ratios of rFNR-3D per PC hexamer (rFNR-3D:$(\alpha^{PC}\beta^{PC})_6$) after gradient analysis were 0.14 ± 0.02 and 0.27 ± 0.015, respectively. Under the same conditions, the PC $(\alpha^{PC}\beta^{PC})_6-(L_{RC}^{22})_1$ linker complex exhibited a higher affinity for the enzyme than PC $(\alpha^{PC}\beta^{PC})_6$ alone. The ratios of rFNR-3D per $(\alpha^{PC}\beta^{PC})_6-(L_{RC}^{22})_1$ were found to be 0.21 ± 0.04 and 0.43 ± 0.04, respectively.

The inset in Figure 4A shows the electrophoretograms of isolated PC, before and after the incubation with rFNR-3D. Figure 4B also shows the electrophoretograms of the PC-L_{RC}^{22} linker complex before and after the incubation with rFNR-3D. The stoichiometries of the L_{RC}^{22} linker polypeptide fragment with respect to the PC $(\alpha\beta)$ protomers are consistent with the assignment of this complex as a hexamer: $(\alpha^{PC}\beta^{PC})_6-(L_{RC}^{22})_1$. The binding assays and analyses described previously indicate that up to one rFNR-3D can bind to such complexes and that the PC-L_{RC}^{22} complex has a higher affinity for FNR than PC hexamers alone.

It is important to note that the enzyme preparation used for the binding experiments to the PC-L_{RC}^{22} linker complex

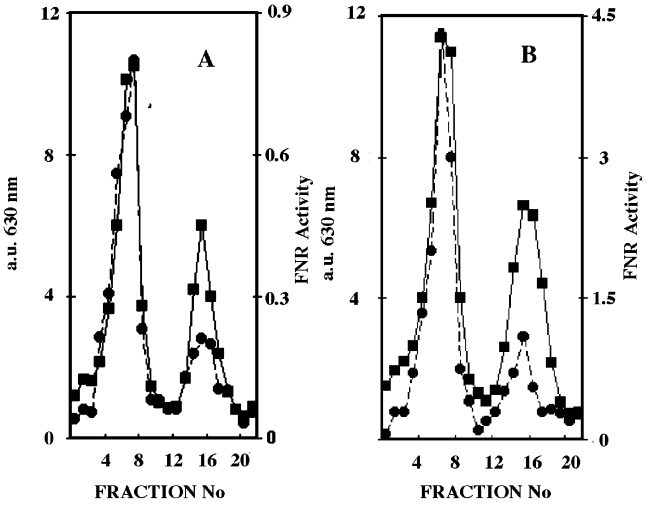

FIGURE 5: Sucrose density gradient analysis of whole-cell extracts from the *cpcC* mutant of *Synechococcus* sp. PCC 7002 after solubilization with Triton X-100. Panel A shows the properties of fractions of the sucrose gradient with PBS from the *cpcC* mutant. In panel B, 6.9 nmol of rFNR-3D was incubated with the same amount of extract prior to loading on the sucrose gradient. The diaphorase activity (●) is plotted as μmol of DCPIP min^{-1} mL^{-1}, and the absorbance units (a.u.) at 630 nm (■) of each fraction are indicated.

and PC hexamers was the same. The enzyme aliquots added to each solution were identical, and the experiments were conducted in parallel. However, the turnover number obtained for the enzyme in the presence of the $(\alpha^{PC}\beta^{PC})_6-(L_{RC}^{22})_1$ linker complex was consistently 1.3−1.5-fold higher than that for the enzyme bound to PC hexamers that did not contain a linker polypeptide. Studies are currently in progress to explore this observation further.

Sucrose Gradient Centrifugation Analysis of Whole-Cell Extracts from cpcC Mutant Cells After Triton X-100 Solubilization. PBS from the *cpcC* mutant contain peripheral rod substructures composed of a single disk of hexameric PC (Figure 1C), as opposed to the two PC hexamers typically found in the rods of wild-type PBS as shown in Figure 1A. Although only one PC hexamer is missing from the peripheral rods, two PC-associated linker polypeptides, L_R^{33} and L_R^9 (compare Figure 1A with 1C), are missing from the PBS of the *cpcC* mutant. Each of these linkers contains a region that is similar in sequence to the N-terminal domain of FNR-3D (see Figure 3). The L_R^{33} linker polypeptide is required for binding a second hexameric PC disk to each peripheral rod (see Figure 1A). The L_R^9 linker is the rod-capping linker (Figure 1A), which limits the rod elongation by preventing the binding of additional PC-L_R^{33} complexes to the peripheral rods and which thereby causes the average rod length to be only two PC hexamers in wild-type PBS (*18*). Accordingly, it could be expected that the binding of the L_R^9 linker would also block the binding of FNR-3D to the peripheral rods. The absence of both linkers from the PBS of the *cpcC* mutant is thus predicted to allow a much greater amount of rFNR-3D to be bound to such PBS when compared to wild-type PBS.

A representative sedimentation pattern from the PBS of the *cpcC* mutant cells is shown in Figure 5A. Diaphorase activity (circles) and absorbance at 630 nm (squares) were plotted for each fraction recovered from the sucrose gradient. Two peaks were clearly distinguished in the 630 nm absorbance profile, and the faster sedimenting fraction contained the PBS (*19*). When a careful comparison is made between the sedimentation profile of extracts from the wild type and the *cpcC* mutant, the more slowly sedimenting fraction in the wild-type extract can be seen to sediment further than the same fraction in the *cpcC* mutant. By using the molecular mass markers aldolase (158 kDa) and catalase (232 kDa), it was shown that this fraction corresponds to PC hexamers in the wild type, while in the *cpcC* mutant this peak corresponds to PC trimers (data not shown). The PBS-containing zone had ~87% of the total absorbance at 630 nm in the gradient for the wild type, but this zone in the *cpcC* mutant gradient contained only 61% of the total 630 nm absorbance. As noted previously, 78% of the FNR derived diaphorase activity in the wild-type extract was bound to the PBS. However, in the *cpcC* extract, 84% of the FNR diaphorase activity is found in the PBS fraction. Thus, the PBS of the *cpcC* mutant, which contain peripheral rods with only one PC hexamer, can still bind FNR-3D at least as effectively as wild-type PBS. These observations are consistent with the observed interactions between rFNR-3D and the $(\alpha^{PC}\beta^{PC})_6-(L_{RC}^{22})_1$ linker complexes as described previously.

The basal level of FNR activity associated with the PBS of the *cpcC* mutant did not differ significantly from that of wild-type PBS. However, when excess rFNR-3D was incubated with a WCE derived from the *cpcC* mutant, an approximately 6-fold increase in the enzyme activity associated with the PBS fraction was observed (Figure 5B; note the change in the scale for FNR activity as compared to Figure 5A). This difference in the binding behavior of rFNR-3D to PBS of the wild type and *cpcC* mutant strains indicates that there are no more than two sites available for FNR-3D binding to the wild-type PBS, which correspondingly must have at least four sites blocked by L_R^9. In the PBS from the *cpcC* mutant, which contain L_{RC}^{27} but are lacking L_R^{33} and L_R^9, six sites are available for FNR-3D binding (as illustrated in Figure 1B).

Sucrose Gradient Centrifugation Analysis of Whole-Cell Extracts from cpcD3 Mutant Cells Solubilized with Triton X-100. The PBS of the *cpcD3* mutant strain lack the L_R^9 linker polypeptide (*18*). Electron microscopic analyses of PBS of this mutant showed that the number of PC hexamers in individual peripheral rod substructures was more variable than in the wild-type PBS. Hence, it was concluded that L_R^9 binds to the core distal face of hexamers containing the L_R^{33} linker polypeptide to prevent the tandem joining of PC hexamers containing the L_R^{33} linker (ref *18*, also see Figure 1C). The sedimentation profiles of WCEs from the *cpcD3* mutant did not differ significantly from the wild-type extracts, either in the absorbance profiles at 630 nm or the diaphorase activity profile (compare Figures 2A and 6A). However, after the WCE from the *cpcD3* mutant was mixed with rFNR-3D, the sedimentation profile showed that the amount of enzyme incorporated by PBS was nearly six times greater than that of wild-type PBS (see Figure 6B). The concentration of PBS in the experiments shown in Figures 1, 5, and 6 are different. The differences in the absorbance scales of these figures are largely due to the difference in the molar extinction coefficients for the PBS of the wild type and *cpcC* and *cpcD3* mutant strains (see Experimental Procedures). For example, the molar extinction coefficient at 630 nm of the

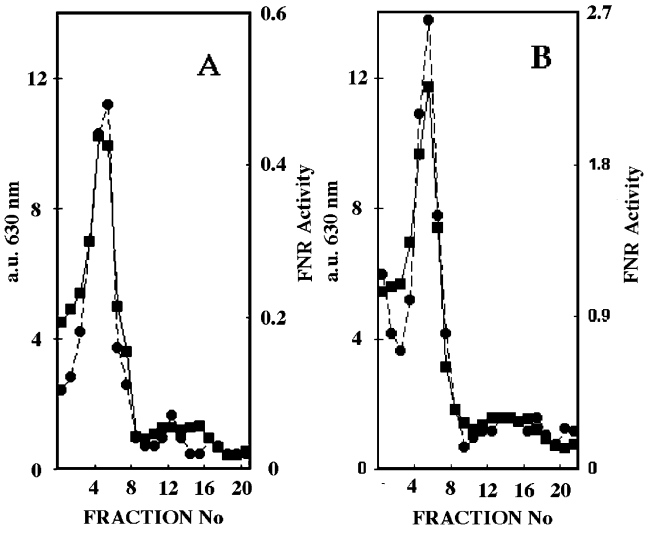

FIGURE 6: Sucrose density gradient analysis of whole-cell extract from the *cpcD3* mutant of *Synechococcus* sp. PCC 7002. Panel A shows the properties of fractions from the sucrose gradient of PBS from the *cpcD3* mutant. In Panel B, 6.9 nmol of rFNR-3D was incubated with the same amount of extract as in panel A prior to sucrose gradient centrifugation. The diaphorase activity (●) is plotted as μmol of DCPIP min^{-1} mL^{-1}, and the absorbance units (a.u.) at 630 nm (■) of each fraction are indicated.

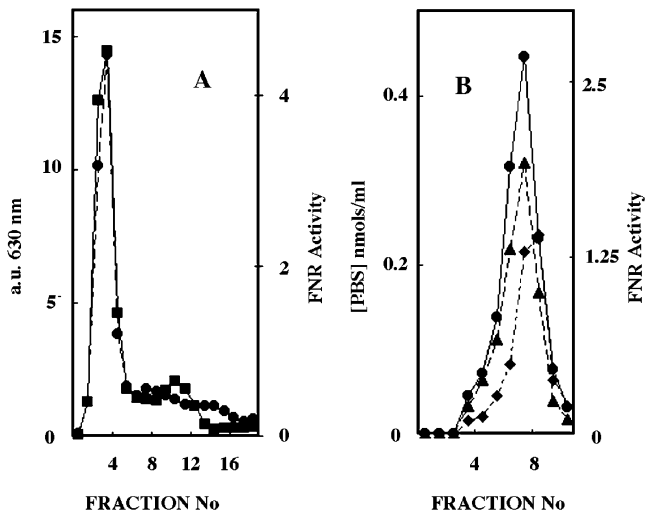

FIGURE 7: Sucrose density gradient analysis of a competition-binding experiment for FNR-3D and a mixture of PBS isolated from the *cpcC* and *cpcD3* mutants of *Synechococcus* sp. PCC 7002. WCE from the *cpcD3* mutant (OD_{630} = 12.2; 14.2 mL) and WCE from the *cpcC* mutant (OD_{630} = 12.3; 10.1 mL) were mixed. This mixture was incubated with 3.45 nmol of rFNR-3D and aliquoted (4 mL) onto sucrose density gradients. Panel A shows the FNR activity (●), plotted as μmol of DCPIP min^{-1} mL^{-1}, and the absorbance units (a.u.) at 630 nm (■) of the fractions are obtained from one of these gradients. The PBS fractions were collected from four of these gradients, pooled, dialyzed against 0.65 M Na^+/K^+-phosphate, and applied to a second sucrose gradient that was centrifuged for only 5 h. Panel B: samples from this second gradient were collected and assayed for FNR activity and absorbance at 630 and 650 nm. Panel B shows the PBS concentrations (nmol of PBS mL^{-1}) for each fraction; the amount of each type of PBS was calculated from the absorbance profile as described in the Experimental Procedures. The concentration of PBS from the *cpcD3* mutant (▲) and from the *cpcC* mutant (◆) are shown for the first 11 fractions from the gradient together with the diaphorase activity (●), expressed as μmol of DCPIP min^{-1} mL^{-1}.

PBS of the *cpcD3* mutant is 1.7-fold greater than that for the PBS of the *cpcC* mutant. PBS from both the *cpcD3* mutant and the *cpcC* mutant lack the L_R^9 linker and are able to bind up to six rFNR-3D per PBS (Figure 1B,C). However, the PBS from the *cpcC* mutant and PBS from the *cpcD3* mutant differ in the manner by which they interact with rFNR-3D. In the PBS of the *cpcC* mutant, the PC complex that is available in the peripheral rods to bind FNR-3D is $(\alpha^{PC}\beta^{PC})_6-(L_{RC}^{27})_1$, while in the PBS of the *cpcD3* mutant, it is the $(\alpha^{PC}\beta^{PC})_6-(L_R^{33})_1$ complex that is available. To assess whether these two types of complexes differ in their binding affinity for FNR-3D, competition-binding experiments were performed as described next.

Competition Binding Experiments of FNR-3D to Phycobilisomes from the cpcC and cpcD3 Mutants. To establish the relative affinity of FNR-3D for PBS of the *cpcC* and *cpcD3* mutants, equimolar concentrations of both types of PBS were mixed and incubated with 6.9 nmol of rFNR-3D. After sucrose gradient centrifugation and fraction, the activity profile overlaps nicely with the 630 nm absorbance profile of the PBS, and ~80% of the added rFNR-3D was incorporated into the two types of PBS. To establish the distribution of the enzyme between the two types of PBS, the concentration of each type was calculated, and the FNR activity was plotted against the fraction number. As expected, PBS from the *cpcD3* mutant sedimented more rapidly than PBS from the *cpcC* mutant. The FNR activity was higher in the PBS fraction that was more rapidly sedimenting; thus, the ratio of FNR per PBS was higher for PBS of the *cpcD3* mutant than for PBS of the *cpcC* mutant (data not shown). To determine more precisely the relative affinity of the PBS from the *cpcC* and *cpcD3* mutant strains for FNR-3D, an analysis of sucrose gradient fractions by SDS−PAGE and densitometry was performed.

A mixture of the two types of PBS and a limiting amount of enzyme was again subjected to sucrose density gradient fractionation. A very narrow peak of FNR activity and 630 nm absorbance was obtained (Figure 7A). Fractions 3 and 5 were chosen for SDS−PAGE and densitometric analyses, and the results are shown in Figure 8. The mixed PBS fractions from four individual centrifuge tubes were pooled and dialyzed against 0.65 M Na^+/K^+-phosphate buffer pH 8.0. The PBS from the pooled fraction were precipitated with 240 mg of ammonium sulfate mL^{-1}, and the PBS were resuspended in the same buffer before application to a second sucrose gradient to improve the PBS separation. The FNR activity and the calculated distribution of PBS from the two mutant strains are shown in Figure 7B. The enzyme activity associated with the more rapidly sedimenting PBS from the *cpcD3* mutant was greater than that associated with the more slowly sedimenting PBS from the *cpcC* mutant. Fractions 7 and 9 were selected for SDS−PAGE and densitometric analyses.

PBS from the wild-type strain and from the *cpcC* and *cpcD3* mutant strains and the two mixtures of PBS from the latter two strains were analyzed by SDS−PAGE (Figure 8 and Table 1). As expected, PBS from the *cpcC* mutant did not contain the L_R^{33} and L_R^9 linker polypeptides (Figure 8, compare lane 3 with lanes 1 and 2), while PBS from the *cpcD3* mutant (Figure 8, lane 4) only lacked the L_R^9 linker polypeptide. The polypeptide compositions of the PBS from *Synechococcus* sp. PCC 7002 wild-type strain and the *cpcC* and *cpcD3* mutant strains were also analyzed quantitatively by densitometric analysis of the SDS−PAGE gel. The

Table 1: Calculated Subunit Stoichiometries for Phycobilisomes Before and After Incubation with Exogenous rFNR-3D[a]

	W.T. PBS	*cpcC* mutant PBS	*cpcD3* mutant PBS	f #3[b] figure 7A	f #5 figure 7A	f #7 figure 7B	f #9 figure 7B
L_{CM}^{99}	1.8	2.1	1.85	1.84	1.78	1.61	1.72
FNR-3D	1.17	1.06	0.93	3.2	1.86	2.43	2.05
L_R^{33}	7.2	0	7.8[c]	6.4	1.67	5	2.6
L_{RC}^{27}	6[a]	6	6	6	6	6	6
PBP[d]		134	245	227	181	230	180
$L_R^9 + L_C^8$	10.2	5.5	5.25	6.3	6.4	5.8	5.2
% *cpcD*3 mutant PBS[c]			100	82	21	64	33
% *cpcD*3 mutant PBS[e]				76	23	73	42

[a] The number of subunits was obtained by densitometric analysis of SDS−PAGE gels as described in the Experimental Procedures. The calculated stoichiometries are the average of two electrophoretograms loaded with 50 and 100 μg of protein per sample, respectively. The data were normalized by assuming that there are six copies of the L_{RC}^{27} linker per PBS. The PBS analyzed from the *cpcC* and *cpcD3* mutant strains was the same PBS used for the competition experiments. [b] f #*x* indicates the fraction number from the figure indicated. [c] An average of 7.8 subunits of L_R^{33} per PBS was obtained for PBS from the *cpcD3* mutant. This value should thus be found for any fraction containing 100% PBS of this type. By determining the ratio of content of this linker protein in various mixtures to this value, the percent composition of PBS from the *cpcD3* mutant can thus be estimated. [d] Values for PBP are approximate and represent the total number of α and β subunits of all phycobiliprotein types. [e] Percent content of PBS from the *cpcD3* mutant estimated from absorbance data.

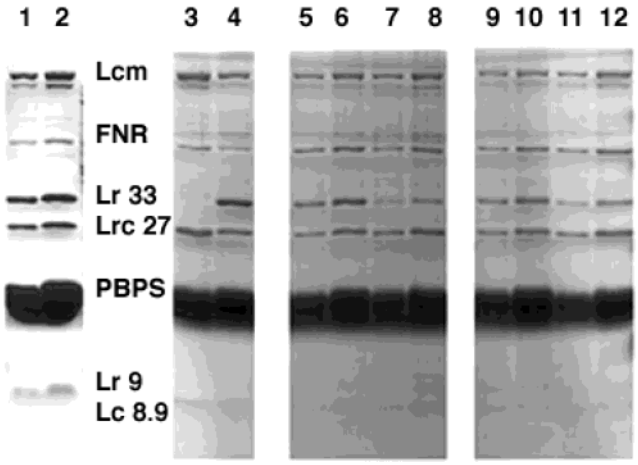

FIGURE 8: SDS−PAGE analysis of fractions from sucrose density gradient analyses of various PBS preparations and from the binding competition experiments. Lanes 1 and 2 contain wild-type PBS (50 and 100 μg of protein, respectively). Lane 3 contains PBS (100 μg protein) from the *cpcC* mutant. Lane 4 contains PBS (50 μg protein) from the *cpcD3* mutant. Lanes 5 and 6 contain PBS (50 and 100 μg of protein, respectively) from fraction 3 (Figure 7A). Lanes 7 and 8 contain PBS (50 and 100 μg of protein, respectively) from fraction 5 (Figure 7A). Lanes 9 and 10 contain PBS (50 and 100 μg of protein, respectively) from fraction 7 (Figure 7B). Lanes 11 and 12 contain PBS (50 and 100 μg of protein, respectively) from fraction 9 (Figure 7B). Polypeptides are identified with labels between lanes 2 and 3.

calculated stoichiometries of the PBS components for the wild type, the *cpcC* mutant, the *cpcD3* mutant, and fractions from the competition binding experiments shown in Figure 7A,B are presented in Table 1. The PBS analyzed in Figure 8 and Table 1 for the *cpcD3* and *cpcC* mutant strains were the same PBS as those used for the experiments in Figure 7A,B. For the mixtures derived from the experiments shown in Figure 7A,B, the content of the PBS from the *cpcD3* strain in each fraction can be directly calculated from the content of the L_R^{33} linker. The mixtures that were enriched for the L_R^{33} also had higher contents of FNR-3D. This can be illustrated by the following stoichiometric ratios: for fraction 3, the ratio of FNR-3D to the L_R^{33} linker is 3.2:6.4, while this ratio was 1.86:1.67 for fraction 5, which contains a higher proportion of PBS from the *cpcC* mutant. The percentage of PBS from the *cpcD3* mutant in fraction 3 was estimated to be 82% by densitometry. This value is in good agreement with the 76% value estimated from the absorbance profile data. Correspondingly, densitometric analyses and absorbance profile estimates for the content of PBS from the *cpcD3* mutant in fraction 9 were 21 and 23%, respectively. Using the information from these densitometric analyses, the distribution of FNR-3D between the two types of PBS could be calculated from simultaneous equations. From the data in Figure 8 (lanes 5−8), a content of approximately four FNR-3D molecules per PBS from the *cpcD3* mutant and about 1.3 FNR-3D molecules per PBS from the *cpcC* mutant could be calculated. The calculated values from the analysis of lanes 9 and 10 of Figure 8 were approximately three FNR-3D molecules per PBS from the *cpcD3* mutant and 1.6 FNR-3D per PBS from the *cpcC* mutant strain.

The FNR distribution was also determined by similar densitometric methods in an experiment in which the molar ratio of PBS from the *cpcC* and *cpcD3* mutants was 3:1 (data not shown). Even under these highly unfavorable binding conditions for the PBS from the *cpcD3* mutant, high ratios of FNR per PBS were observed in L_R^{33}-enriched fractions. These data confirmed that PC hexamers associated with the L_R^{33} linker have a higher affinity for FNR-3D than PC hexamers associated with the L_{RC}^{27} linker polypeptide.

DISCUSSION

A previous study by van Thor et al. (*14*) concluded that FNR is bound to PBS via the core-proximal hexamer of PC in *Synechocystis* sp. PCC 6803, and these authors further concluded that FNR is not bound at the core-distal binding sites on PC that are normally occupied by CpcD. The results presented here show very clearly that their model suggesting that FNR is somehow bound to wild-type PBS through an interaction with the $(\alpha^{PC}\beta^{PC})_6-L_{RC}^{27}$ complex is not correct. Although FNR-3D certainly can bind to core-proximal $(\alpha^{PC}\beta^{PC})_6-L_{RC}^{27}$ complexes in PBS isolated from a *cpcC* mutant strain, the peripheral rod complexes containing this linker protein are shown here to be identical since up to six binding sites for FNR-3D are available in such PBS. The very same situation is found for PBS from a mutant lacking only CpcD; these PBS also can bind a maximum of six FNR-3D molecules per PBS. However, this is clearly not the case in wild-type PBS, for which a maximum of two FNR-3D

molecules can be bound per PBS. These observations, as well as the *in vitro* binding studies of FNR-3D with PC complexes (see below), show that, while FNR-3D can bind to the core-proximal $(\alpha^{PC}\ \beta^{PC})_6-L_{RC}^{27}$ complex, it is not bound in this manner in PBS isolated from the wild type or the *cpcD3* mutant strain of *Synechococcus* sp. PCC 7002. If FNR-3D was binding to a site other than that normally occupied by either the C-terminal domain of CpcC or the CpcD protein, then this site should be available for binding additional FNR-3D molecules in wild-type PBS, but such binding was clearly not observed. It is an open question whether FNR could bind to APC in a mutant unable to synthesize the L_C^8 core linker, ApcC, which has much lower sequence similarity to CpcD.

Nakajima et al. (*11*) were the first to show a direct interaction between FNR and PC by purifying a complex of the two proteins, although the exact stoichiometry between FNR and PC was not determined, and the size of the purified complex was estimated to be only 78 kDa. It is shown here that FNR-3D can bind to PC hexamers but that the binding affinity of FNR-3D is somewhat greater to a $(\alpha^{PC}\ \beta^{PC})_6-L_{RC}^{22}$ linker complex. However, binding-competition studies between PBS of a *cpcC* mutant and those from a *cpcD* mutant of *Synechococcus* sp. PCC 7002 show that peripheral rods containing CpcC (L_R^{33}) have a higher affinity for FNR than peripheral rods containing only CpcG (L_{RC}^{27}). Therefore, one can conclude that the relative binding affinities of FNR-3D for PC complexes has the following order: $(\alpha^{PC}\ \beta^{PC})_6-L_R^{33} > (\alpha^{PC}\ \beta^{PC})_6-L_{RC}^{27} > (\alpha^{PC}\ \beta^{PC})_6$. Given this order of affinities, FNR is most likely bound to core-distal $(\alpha^{PC}\ \beta^{PC})_6-L_R^{33}$ complexes that are not capped by CpcD.

As shown in the studies presented here and as noted above, FNR-3D can bind to PC hexamers that include a 22-kDa fragment derived from L_{RC}^{27}. Such complexes would normally associate with a second PC hexamer through an interaction with the C-terminus of CpcC, the L_R^{33} linker. Evidently, the CpcD-like domain of FNR-3D, which clearly has strong sequence similarity to the C-terminus of CpcC (Figure 3) as well as CpcD, can bind to the toroid-shaped PC trimer whose central cavity is not blocked by its interaction with CpcG (L_{RC}^{27}). This observation is interesting since CpcD either does not bind to such complexes or binds with much lower affinity and is lost during the preparation of PBS from the *cpcC* mutant strain. Similar results can be observed for the PMB2 mutant of *Synechocystis* sp. PCC 6803, whose PBS include FNR and the L_{RC}^{27} linker but lack CpcD and two peripheral rod linkers of 33 and 35 kDa (*39*). Therefore, our findings suggest that FNR could bind to PC complexes as the PBS are being assembled but that this process is controlled by a competition determined by the relative affinity of FNR-3D for each trimer of PC and the phycobiliprotein linkers.

Two major questions remain regarding the CpcD domain of FNR-3D: when and why did this extra CpcD-like domain evolve? Nearly all characterized cyanobacteria that employ phycobiliproteins organized into PBS as their light harvesting antennae have *petH* genes that encode an N-terminal, CpcD-like domain. However, an interesting exception to this observation is found in *Gloeobacter violaceus* PCC 7421 (*40*). On the basis of the absence of thylakoid membranes and its 16S rRNA sequence, *G. violaceus* PCC 7421 is believed to have diverged very early from the remainder of the cyanobacterial lineage. Interestingly, its *petH* gene (S. Tabata and T. Kaneko, personal communication) predicts an FNR protein of only 296 amino acids, and no CpcD-like domain is present at its N-terminus. The *petH* gene of *G. violaceus* encodes only the two catalytic domains; this situation is similar to that for the FNR of chloroplasts and cyanelles (see below). One possibility is that *G. violaceus* diverged from the ancestor(s) of most other cyanobacteria prior to the evolutionary event that fused a *cpcD*-like gene at the 5′ end of the *petH* gene. Phylogenetic analyses of FNR sequences (data not shown) are consistent with this possibility.

Another interesting case is found in the living fossil, *Cyanophora paradoxa*, which is a biflagellated eukaryotic protist that harbors peptidoglycan-surrounded plastids called cyanelles (*41*). Like most cyanobacteria, cyanelles synthesize phycobiliproteins that form hemidiscoidal PBS (*42*). The FNR of *C. paradoxa* is encoded in the nucleus rather than the cyanelle, and the protein is synthesized as a larger precursor with a plastid import sequence that is capable of directing the protein into pea chloroplasts (*43*). However, this FNR lacks the CpcD-like domain of cyanobacterial FNR proteins and thus is unlikely to be associated with the PBS. It is possible that the cyanobacterium, which was the ancestor of the endosymbionts that evolved into cyanelles and chloroplasts, did not possess FNR with a CpcD-like domain. This could actually have been a later development in cyanobacterial descendants of that ancestral organism, and this improvement might have then been passed down to the ancestors of all extant cyanobacteria. Alternatively, the cyanobacterial ancestor of cyanelles and chloroplasts might have had an FNR with a CpcD-like domain that was lost when the *petH* gene was transferred to the nucleus or that was rapidly and extensively modified to become the chloroplast/cyanelle import sequence. Since FNR of higher plant chloroplasts can be isolated in a complex with the cytochrome b_6f complex (*24*), it would be interesting to know whether this is also the case with the FNR in the cyanelles of *C. paradoxa* and in the chloroplasts of red algae.

A very interesting and relevant situation is found in *Prochlorococcus marinus*. *P. marinus* is very closely related to some marine *Synechococcus* sp., including *Synechococcus* sp. WH8102, but *P. marinus* differs from true cyanobacteria by not producing PBS and by using chlorophyll proteins as light harvesting antennae, although some strains can synthesize small amounts of PBP (*44*). FNR of *P. marinus* has an N-terminal extension that is shorter than the CpcD-like domains of cyanobacteria. While this domain bears relatively little sequence similarity to the CpcD-like domains of most cyanobacterial FNR proteins, it has a somewhat greater level of similarity (~30%) to the CpcD-like domain of *Synechococcus* sp. WH8102 FNR (Figure 3). It seems that the N-terminal domain of *P. marinus* FNR is rapidly diverging from the sequence of its close relative, *Synechococcus* sp. WH8102, and from those of other cyanobacteria. The vestiges of a CpcD-like domain are still recognizable, but since *P. marinus* has no PBS, the sequence has diverged to become shorter and is extensively modified. It should be clear from this discussion that FNR sequences are potentially interesting evolutionary markers for both ancient and recent cyanobacterial evolution. Future studies may reveal whether the ancestor of chloroplasts and cyanelles diverged before

the fusion of the CpcD-like domain to FNR or whether this feature was lost after the primary endosymbiotic event that led to eukaryotic phototrophs.

The other remaining question pertains to the functionality of this enzyme in cyanobacteria: why should FNR be bound to the peripheral rods of PBS? It was originally proposed that the purpose of this positioning was to maintain the enzyme in close proximity to the stromal surface of the thylakoid membrane to keep FNR close to PS I, the source of reduced ferredoxin (*5*). After the structures of PS I and PS II became available, Bald et al. (*45*) modeled the interactions among the reaction centers and the PBS in cyanobacterial thylakoid membranes, and they proposed two models for interaction of the PBS with PS I. The most sterically favored model was one in which the PBS interacted with PS I via FNR located at the end of the peripheral rods of the PBS rather than a model in which the PBS cores interacted with the PS I trimers. More recently, McConnell et al. (*46*) have performed studies on state transitions and presented a model for state transitions that also takes into account these X-ray structures. Their model also favors an interaction of the PBS with PS I via FNR that is bound to the distal ends of the peripheral rods. Glazer et al. (*47*) found evidence for connections between PBS and PS I when they used *N*-ethylmaleimide to disrupt interactions dependent upon accessible sulfhydryl groups. This treatment only disrupted energy transfer from PBS to PS I, and the only proteins in either complex that appeared to be affected were FNR and CpcD (*47*). As noted previously in the results presented here, the turnover numbers for the PBS- or PC-bound FNR were somewhat larger than for the free enzyme. The structural basis for this enhanced enzymatic activity is not known at present, but nevertheless, it appears that PBS-bound FNR is more active than the free enzyme. van Thor et al. (*14*, *23*) have reported that a *Synechocystis* sp. PCC 6803 mutant, which produces a truncated FNR protein lacking the CpcD-like domain, is unable to adapt to salt stress. The *petH* mRNA levels and PS I-dependent cyclic electron transport activities are normally elevated under salt shock conditions but do not increase in a mutant that produces an FNR lacking the CpcD domain under the same stress conditions. They conclude that FNR requires an interaction with the thylakoid membrane, which is dependent upon the CpcD-like domain, to adapt to high salt stress (*23*). Also, evidence for a membrane-associated form of FNR in the marine cyanobacterium *Synechococcus* sp. PCC 7002 was reported (*5*). However, the location and role of a postulated acylation of FNR has still not been resolved.

Another possible role for the tethering of FNR to the distal ends of the peripheral rods of PBS near the thylakoid membrane is to facilitate its involvement in PS I-mediated cyclic or respiratory electron transport. If one considers that a maximum of two FNR-3D molecules can be bound per PBS in wild-type *Synechococcus* sp. PCC 7002, and if all six peripheral rods are equivalent in their ability to bind FNR-3D, then more than half of the PBS should have at least one FNR bound to those peripheral rods adjacent to the thylakoid membrane surface, and 6.6% of the PBS would have both enzymes in close contact with the membrane surface. This amount of FNR would be sufficient for the observed levels of cyclic electron transport, and it is possible that these enzymes might be able to participate in the direct reduction of plastoquinone with electrons from ferredoxin. The calculated pI of the CpcD-like domain of cyanobacterial FNR is ~10, and the net positive charge is larger in the hinge region. Thus, if there is an additional binding interaction between FNR and a protein (e.g., through a PS I subunit) or the lipids of the thylakoid membranes, then it is possible that an even greater proportion of the FNR would be bound to the peripheral rods in closest proximity to the thylakoid membrane. This might facilitate a ternary interaction between FNR, PS I, and ferredoxin as has been suggested (*14*).

We have measured the FNR-mediated oxidation of NADPH in the presence of benzoquinones and naphthoquinones, which are excellent electron acceptors (data not shown). Thus, it is certainly possible that FNR has a quinone reductase activity, and the crucial point is whether FNR-3D is able to perform its electron-transfer reactions at the membrane interface between the lipid and the aqueous environment. It has been suggested that the interaction of PBS with the thylakoid membrane also occurs via multiple, weak interactions with lipid headgroups (*48*).

Plastoquinone is found in the thylakoid membrane and is highly hydrophobic because of its C-45 isoprenoid tail. Any transfer of electrons from FAD to plastoquinone would have to occur in a surface-accessible pocket that is shielded from bulk solvent water. The PQ molecule would have to leave the lipid bilayer, at least partially, to reach the catalytic site of FNR-3D by facilitated diffusion into this hydrophobic channel. Interestingly, a hydrophobic cavity in FNR has been described for both the spinach as well as the *Anabaena variabilis* enzymes (*3*, *49*). This cavity is sufficiently large to accommodate the headgroup of plastoquinone. Whether other membrane components are required to allow such an interaction to occur is an intriguing but unresolved question.

If it should be important for FNR to be near the thylakoid membrane, as appears to be the case in chloroplasts, one difference between chloroplasts and cyanobacteria is the site of FNR attachment (the cytochrome b_6f complex vs the PBS). Although specific interactions with these two macromolecular assemblies might be sufficient for FNR localization, it remains possible that electrostatic interactions between FNR and thylakoid surface are also important in this localization. In *P. marinus*, the N-terminal domain of FNR has a net positive charge of nine. Within the N-terminal 74 amino acids, there are 10 positive and five negative charges within the first 60 amino acids, and there are five positive and one negative charges from residues 61 to 74. The high content of positive charge implies that the protein would exhibit strong electrostatic interactions with polyanions. Thus, it is possible that *P. marinus* FNR could associate with the thylakoid membrane via electrostatic interactions with anionic lipids of the membrane. *G. violaceus* PCC 7421 has bundle-shaped PBS that are 50−70 nm long (*50*); if FNR were attached to the thylakoid-distal ends of the long phycobiliprotein rods of these PBS by a similar CpcD-like domain, then the FNR would be nearly 75 nm from the thylakoid membrane surface. This may be the reason *G. violaceus* does not have, or never acquired, the CpcD-like domain of FNR. It will be interesting to determine the localization of FNR in *P. marinus* and *G. violaceus*. It will also be interesting to localize FNR in cyanobacterial heterocysts since these specialized cells have very high demands for ATP but have highly reduced PBS contents.

ACKNOWLEDGMENT

The authors thank Drs. E. B. Gutierrez-Cirlos and Nicole Ballew for their revisions and critical reading of the manuscript. The authors also thank Drs. Satoshi Tabata and Takakazu Kaneko of the Kazusa DNA Research Institute for providing the sequence of the *petH* gene of *Gloeobacter violaceus* sp. PCC 7421 prior to publication.

REFERENCES

1. Morand, L. Z., Cheng, R. H., Krogmann, D. W., and Ho, K. K. (1994) in *The Molecular Biology of Cyanobacteria* (Bryant, D. A., Ed.) pp 381−407, Kluwer Academic Publishers, Dordrecht, The Netherlands.
2. Carrillo, N., and Vallejos, R. H. (1987) in *Topics in Photosynthesis* (Barber, J., Ed.) Vol. 8, pp 527−560, Elsevier, Amsterdam, The Netherlands.
3. Karplus, P. A., Daniels, M. J., and Herriot, J. R. (1991) *Science 251*, 60−66.
4. Aliverti, A., Ferioli, C., Spinola, M., Raimondi, D., Zanetti, G., Finnerty, C., Faber, R., and Karplus, P. A. (1999) in *Flavins and Flavoproteins, Proceedings of 13th International Symposium* (Ghisla, S., Kroneck, P., Macheroux, P., and Sund, H., Eds.) pp 265−268, Rudolf Weber, Berlin, Germany.
5. Schluchter, W. M., and Bryant, D. A. (1992) *Biochemistry 31*, 3092−3102.
6. van Thor, J. J., Hellingwef, K. J., and Matthijs, C. P. (1998) *Plant Mol. Biol. 36*, 353−363.
7. Gómez-Lojero, C., Pérez-Gómez, B., and Falcon, M. A. (1998) *IX International Symposium on Phototrophic Prokaryotes*, p 128, Vienna, Austria.
8. Schluchter, W. M. (1994) Ph.D. Thesis, The Pennsylvania State University, University Park, PA.
9. Martínez-Júlvez, M., Hurley, J. K., Tollin, G., Gómez-Moreno, C., and Fillat, M. F. (1996) *Biochim. Biophys. Acta 1297*, 200−206.
10. Kaneko, T., Sato, S., Kotani, H., Tanaka, A., Asamizu, E., Nakamura, Y., Miyajima, N., Hirosawa, M., Sugiura, M., Sasamoto, S., Kimura, T., Hosouchi, T., Matsuno, A., Muraki, A., Nakazaki, N., Naruo, K., Okumura, S., Shimpo, S., Takeuchi, C., Wada, T., Watanabe, A., Yamada, M., Yasuda, M., and Tabata, S. (1996) *DNA Res. 3*, 109−136.
11. Nakajima, M., Sakamoto, T., and Wada, K. (2002) *Plant Cell Physiol. 43*, 484−493.
12. Fillat, M. F., Flores, E., and Gómez-Moreno, C. (1993) *Plant Mol. Biol. 22*, 725−729.
13. Kaneko, T., Nakamura, Y., Wolk, C. P., Kuritz, T., Sasamoto, S., Watanabe, A., Iriguchi, M., Ishikawa, A., Kawashima, K., Kimura, T., Kishida, Y., Kohara, M., Matsumoto, M., Matsuno, A., Muraki, A., Nakazaki, N., Shimpo, S., Sugimoto, M., Takazawa, M., Yamada, M., Yasuda, M., and Tabata, S. (2001) *DNA Res. 8*, 205−213.
14. van Thor, J. J., Gruters, O. W. M., Matthijs, H. C. P., and Hellingwerf, K. J. (1999) *EMBO J. 18*, 4128−4136.
15. Reuter, W., Wiegand, G., Huber, R., and Than, M. E. (1999) *Proc. Natl. Acad. Sci. U.S.A. 96*, 1363−1368.
16. Sidler, W. A. (1994) in *The Molecular Biology of Cyanobacteria* (Bryant, D. A., Ed.) pp 139−216, Kluwer Academic Publishers, Dordrecht, The Netherlands.
17. Bryant, D. A. (1991) in *Cell Culture and Somatic Cells Genetics of Plants*, Vol. 7B: The molecular biology of plastids and mitochondria (Bogorad, L., and Vasil, I. K., Eds.) pp 255−298, Academic Press Inc., New York.
18. de Lorimier, R., Bryant, D. A., and Stevens, S. E., Jr. (1990) *Biochim. Biophys. Acta 1019*, 29−41.
19. de Lorimier, R., Gugliemi, G., Bryant, D. A., and Stevens, S. E., Jr. (1990) *Arch. Microbiol. 153*, 541−549.
20. Bryant, D. A., Stirewalt, V. L., Glauser, M., Frank, G., Sidler, W., and Zuber, H. (1991) *Gene 107*, 91−99.
21. González de la Vara, L., and Gómez-Lojero, C. (1986) *Photosynth. Res. 8*, 65−78.
22. Scherer, S., Alpes, I., Sadowski, H., and Boger, P. (1988) *Arch. Biochem. Biophys. 267*, 228−235.
23. van Thor, J. J., Jeanjean, R., Havaux, M., Sjollema, K. A., Joset, F., Hellingwerf, K. J., and Matthijs, H. C. P. (2000) *Biochim. Biophys. Acta 1457*, 129−144.
24. Zhang, H., Whitelegge, J. P., and Cramer, W. A. (2001) *J. Biol. Chem. 276*, 38159−38165.
25. Stevens, S. E., Jr., and Porter, R. D. (1980) *Proc. Natl. Acad. Sci. U.S.A. 77*, 6052−6056.
26. Bryant, D. A., de Lorimier, R., Guglielmi, G., and Stevens, S. E., Jr., (1990) *Arch. Microbiol. 153*, 550−560.
27. Sancho, J., Peleato, M. L., Gómez-Moreno, C., and Edmonson, D. E. (1988) *Arch. Biochem. Biophys. 260*, 200−207.
28. Yu, M. H., Glazer, A. N., and Williams, R. C. (1981) *J. Biol. Chem. 256*, 13130−13136.
29. Shin, M. (1971) *Methods Enzymol. 23*, 440−447.
30. Schgger, H., and von Jagow, G. (1987) *Anal. Biochem. 166*, 368−379.
31. Gómez-Lojero, C., Pérez-Gómez, B., Prado-Flores G., Krogmann D. W., Cárabez-Trejo, A., and Peña-Díaz, A. (1997) *Int. J. Biochem. Cell Biol. 29*, 1191−1205.
32. Fuglistaller, P., Suter, F., and Zuber, H. (1985) *Biol. Chem. Hoppe-Seyler 366*, 993−1001.
33. Kalla, S. R., Lind, L. K., Lidholm, J., and Gustafsson, P. (1988) *J. Bacteriol. 170*, 2961−2970.
34. Lomax, T. L., Conley, P. B., Schilling, J., and Grossman, A. R. (1987) *J. Bacteriol. 169*, 2675−2684.
35. Mazel, D., and Marliere, P. (1989) *Nature 341*, 245−248.
36. Federspiel, N. A., and Grossman, A. R. (1990) *J. Bacteriol. 172*, 4072−4081.
37. Gray, B. H., Cosner, J., and Gantt, E. (1976) *Photochem. Photobiol. 24*, 299−302.
38. Gottschalk, L. Fischer, R., Lottspeich, F., and Scheer, H. (1991) *Photochem. Photobiol. 54*, 283−288.
39. Elmorjani, K., Thomas, J. C., and Sabban, P. (1986) *Arch. Microbiol. 146*, 186−191.
40. Rippka, R., Waterbury, J. B., and Cohen-Bazire, G. (1974) *Arch. Microbiol. 100*, 419−436.
41. Aitken, A., and Stainer, R. Y. (1979) *J. Gen. Microbiol. 112*, 219−223.
42. Giddings T. H., Jr., Wasmann, C., and Staehelin, L. A. (1983) *Plant Physiol. 71*, 409−419.
43. Jakowitsch, J., Bayer, M. G., Maier, T. L., Luettke, A., Gebhart, U. B., Bohnert, H. J., Schenk, H. E. A., and Löffelhardt, W. (1993) *Plant Mol. Biol. 21*, 1023−1033.
44. Partensky, F., Hess, W. R., and Vaulot, D. (1999) *Microbiol. Mol. Biol. Rev. 63*, 106−127.
45. Bald, D., Kruip, J., and Rogner, M. (1996) *Photosynth. Res. 49*, 103−118.
46. McConnell, M. D., Koop, R., Vasilev, S., and Bruce, D. (2002) *Plant Physiol. 130*, 1201−1212.
47. Glazer, A. N., Gindt, Y. M., Chan, C. F., and Sauer, K. (1994) *Photosynth. Res. 40*, 167−173.
48. Sarcina, M., Tobin, M. J., and Mullineaux, C. W. (2001) *J. Biol. Chem 276*, 46830−46834.
49. Serre, L., Vellieux, F. M. D., Medina, M., Gómez-Moreno, C., Fontecilla-Camps, J. C., and Frey, M. (1996) *J. Mol. Biol. 263*, 20−39.
50. Guglielmi, G., Cohen-Bazire, G., and Bryant, D. A. (1981) *Arch. Microbiol. 129*, 181−189.

BI0346998